25th ABCM International Congress of Mechanical Engineering
October 20-25, 2019, Uberlândia, MG, Brazil

COB-2019-1822
COMPARISON OF DIFFERENT EXCITATION SIGNALS IN A ROTORDYNAMIC SYSTEM

Diego Alejandro Godoy Diaz
David Julian Gonzalez Maldonado
Fernando Augusto de Noronha Castro Pinto
Thiago Gamboa Ritto
Vinicius Ferreira Cortes
Acoustics and Vibrations Laboratory, Federal University of Rio de Janeiro. Av. Horacio Macedo 2030 Centro de Tecnologia bloco i-130, Rio de Janeiro. 21941-914
dgodoy@ufrj.br
david.julian@ufrj.br
fcpinto@ufrj.br
tritto@mecanica.coppe.ufrj.br
viniciuscortes@poli.ufrj.br

Abstract: *This paper deals with the performance of different excitation signals. They are applied to a test rig of active magnetic bearings to identify its stiffness and damping parameters. Experimental results are shown for each parameter obtained at discrete frequencies. Four signals are compared: pure harmonic, sweep, white noise and four low crest-factor multisine signals. Results showed that the dispersion of the parameters' estimates using sweep and white noise signals is high. The lowest dispersion was found with the pure harmonic signal, even though the delayed time where significantly longer than the other assessed waves*

Keywords: *Excitation Signal, Multisine Signal, Active Magnetic Bearings, Parameters Identification*

1. INTRODUCTION

An important step in identification procedure is related to the excitation signal. Due to the noise presence in the field test measurements, the frequency response function (FRF), and therefore, the estimated parameters of a system are susceptible to errors, even when the tests are performed in the same boundary conditions. When the lasted time in a experiment is not important, the well known stepped sine is the best choice, since such signal concentrates the injected energy in only one frequency at a time(Schoukens *et al.*, 2000). The capability of detecting the nonlinear contributions, observed as harmonic multiples of the excited frequency (Schoukens *et al.*, 1988), is also another vantage of such signal.

Systems where the total experiment time is a restriction, the use of stepped sine excitation is no longer feasible. To tackle this problem, alternative signals as *swept*, *binary* or *pseudo-noise* were used in the last decades, due to their availability in the standard signal generator devices. The recent digital to analog converters made possible custom excitation signals, produced by algorithms implemented in order to improve the energy distribution in a system excitation band of frequency.

As an example of a rotordynamic application, an Active Magnetic Bearing system (AMBs), which can control the shaft position as well as produce the excitation signal for identification purposes, is used in this work to assess the performance of different excitation signals. Perhaps one of the first authors to compare the performance of stepped sine and broadband signals was Hynynen (Hynynen, 2011). Such a work also compared the averaging methods, specially for multisine signals. A similar work in a different test rig was made by Khader(Khader *et al.*, 2014), highlighting the better performance of the signals when their crest factor remains low. Vuojolainen et al. (Vuojolainen *et al.*, 2017) compared several excitation signals in a qualitative way in the same AMB test rig where Hynynen performed her experiments. Diaz et al. (Diaz *et al.*, 2017) used a small scale test rig to compare flat multisine signals with different phase configurations. The same authors (Diaz *et al.*, 2018) compared the FRF at several rotation speeds, observing as the previously mentioned authors the beneficial proprieties when the excitation signals are less impulsive (low crest factor), and the influence of FRFs only in the shaft rotating frequency and its multiples due to the unbalancing contributions into the system.

2. IDENTIFICATION PROCEDURE

Basically, in the frequency domain sense, a set of system parameters are obtained firstly exciting the desired frequency band and then measuring its inputs and outputs. Those measurements are transformed in the frequency domain using the discrete Fourier transform (DFT), generally implemented in the Fast Fourier Transform (FFT) algorithm. The ratio of the outputs to the inputs yields to the frequency response function (FRF)Nordmann (1984), as shown in Fig. (1). The FRF matrix is then fitted to a model as will be presented in next subsections.

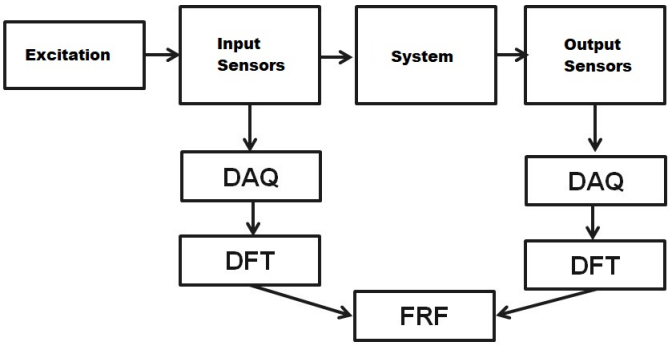

Figure 1: Excitation procedure block diagram Nordmann (1984)

2.1 Active Magnetic Bearing excitation

As proposed in standard ISO 14839-3 (ISO, 2006) and detailed in Schewitzer and Maslen (Schweitzer and Maslen, 2009), the excitation signals s can be added after the controller block (see Fig. (2)). The currents of the coils and the shaft position are measured in order to estimate the magnetic force.

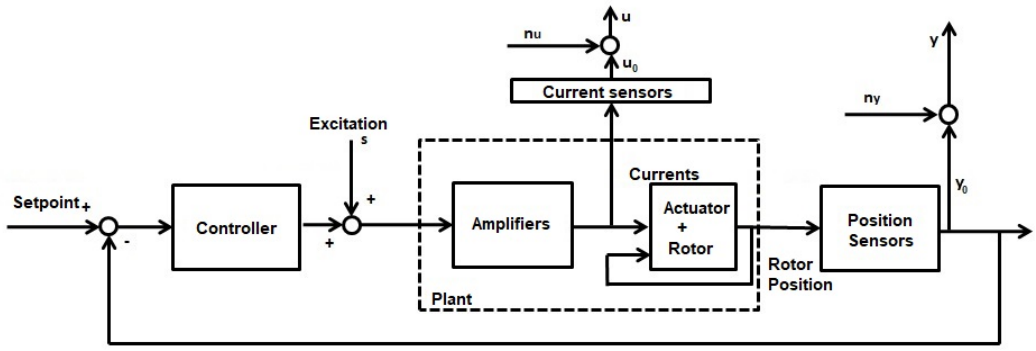

Figure 2: Excitation procedure block diagram in an AMB system

The block excitation diagram can be generalized to a rotordynamic system with electromagnetic actuators, even if there is no AMB supporting the shaft, only removing the controller block and the feedback loop.

2.2 Dynamic Stiffness Matrix

A rotordynamic system can be represented as(Muszynska, 2005):

$$\boldsymbol{M}\ddot{\mathbf{q}} + (\boldsymbol{C} + \Omega \boldsymbol{G})\,\dot{\mathbf{q}} + \boldsymbol{K}\mathbf{q} = \mathbf{f_{ext}}, \tag{1}$$

where $\boldsymbol{M}$, $\boldsymbol{K}$, $\boldsymbol{C}$ e $\boldsymbol{G} \in \mathbb{R}^{4N_e+4\times 4N_e+4}$ are the mass, stiffness, damping and gyroscopic effect, respectively. Vector $\mathbf{f_{ext}}$ represents the applied external forces.

Equation (1), can be expressed in the complex form, as follows:

$$\underbrace{\left[\boldsymbol{K} - \omega^2\boldsymbol{M} + j\omega\boldsymbol{C} - j\omega\Omega\boldsymbol{G}\right]}_{\text{CDS}}\bar{\mathbf{q}}_{\mathbf{u}} = \boldsymbol{H}\bar{\mathbf{q}}_{\mathbf{u}} = \bar{\mathbf{f}}_{\mathbf{u}}, \tag{2}$$

relating the displacement $\mathbf{q} = \bar{\mathbf{q}}_{\mathbf{u}}e^{j\omega t}$ and force $\mathbf{f} = \bar{\mathbf{f}}_{\mathbf{u}}e^{j\omega t}$ vectors in the generalized and complex forms.The

left term is known in literature as Complex Dynamic Stiffness (Nordmann, 1984) or mechanical impedance (San Andres, 2006) of the system.

Aiming to increase the signal-to-noise ratio (SNR), the acquisition is made for N_b periods or *blocks*, and then an averaging procedure is made in order to obtain the CDS matrix H. A detailed survey of such averaging methods, or also called *estimators*, is presented in Guillaume(Guillaume, 1998)(Guillaume, 1992) and VerbobenVerboben (2002). For closed loop systems as AMBs, the instrumental variables estimator (Verboben, 2002), also called as indirect (Guillaume, 1998) or three signals estimator (Wernholt and Moberg, 2008) yields to the best linear approximation(Pintelon and Schoukens, 2001), and is expressed as:

$$\boldsymbol{H_{JIO}}(\omega_k) = \left(\frac{1}{N_b} \sum_{l=1}^{N_b} \boldsymbol{F}(\omega_k)^{(l)} \boldsymbol{S}^*(\omega_k)^{(l)} \right) \left(\frac{1}{N_b} \sum_{l=1}^{N_b} \boldsymbol{Q}(\omega_k)^{(l)} \boldsymbol{S}^*(\omega_k)^{(l)} \right)^{-1}, \tag{3}$$

where $\boldsymbol{F}(\omega_k)^{(l)} = \left[, \bar{\mathbf{f}}_{\mathbf{m,1}}{}^{(l)} \quad \bar{\mathbf{f}}_{\mathbf{m,2}}{}^{(l)} \right]$, $\boldsymbol{Q}(\omega_k)^{(l)} = \left[\bar{\mathbf{q}}_{\mathbf{m,1}}{}^{(l)} \quad \bar{\mathbf{q}}_{\mathbf{m,2}}{}^{(l)} \right]$ e $\boldsymbol{S}^*(\omega_k)^{(l)} = \left[\bar{\mathbf{s}}_{\mathbf{m,1}}{}^{(l)} \quad \bar{\mathbf{s}}_{\mathbf{m,2}}{}^{(l)} \right]^*$ represents the set of complex vectors for the frequency ω_k of the forces, displacements and excitations signals, respectively. The superscript * indicates the complex conjugate of the matrix, and $^{(l)}$ represents the $l-th$ block. Since the displacement is to be considered as planar, at least two different experiments have to be performed in order to avoid the ill-conditioned inverse matrix. It is common to perform first the excitation in the horizontal and then the vertical axis of the shaft.

3. EXCITATION SIGNALS

For this work, general purpose excitation signals were used to compare their performance. Besides those signals, modified signals, which modifies the phases of the initial multisine signal, in order to perform a *compact* process.

3.1 Multisine signal

The multisine or *multitone* signal is the sum of N_f stepped sine waves, expressed as:

$$s(t) = \sum_{k=1}^{N_f} A_k \cos(2\pi f_k t + \phi_k), \tag{4}$$

where A_k, f_k and ϕ_k are the amplitude, the frequency and the phase of the k-th component, respectively.

3.2 Clipping method

The clipping method, proposed by Ouderaa et al.(Van der Ouderaa *et al.*, 1988), consist in the procedure of *cut* a signal, obtain its spectrum, restore de initial magnitude values and rebuild the time domain wave by means of the inverse discrete Fourier transform (IDFT), repeating the latter steps until there is a convergence behavior in the crest factor value, as shown in Fig. (3).

As example, a multisine with 17 components and flat spectrum is shown in Fig. (4). The algorithm preserves the amplitude in the excited frequencies, and modifies the phases. It can be noted the formation of low amplitude harmonics in the spectrum, known in literature Pintelon and Schoukens (2001) as *snow effect*.

The crest factor evolution can be observed in Fig. (5). The convergence is reached after approximately 80 iterations.

3.3 Chebyshev method

The Chebyschev method, proposed by Guillaume et al. (Guillaume *et al.*, 1991), consists in the minimization of the l_∞ norm of a vector, by means of the Levenberg Marquardt approach. The flow diagram is presented in Fig. (6).

4. EXPERIMENTAL RESULTS

A small scale AMB system was employed to perform the experiments with the different excitation signals selected. Seven signals were compared, comprising in three general purpose excitation (stepped sine, sweep and white noise). Four multisine signals, one with random phases, and three modified with the two algorithms previously presented. The initial spectrum amplitudes were also modified in some of the signals in order to excite evenly the displacement frequencies. All the signals are summarized in Tab. (1).

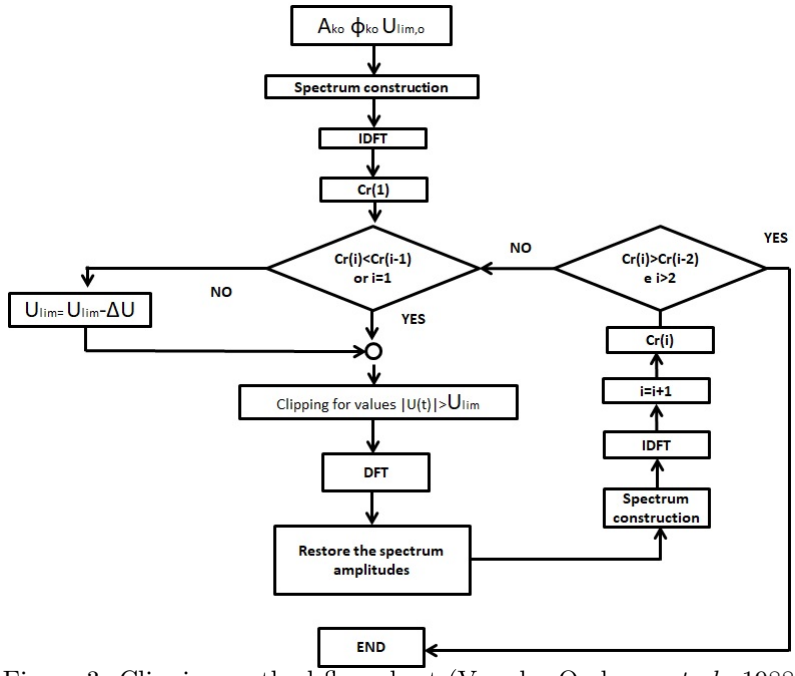

Figure 3: Clipping method flow chart (Van der Ouderaa *et al.*, 1988)

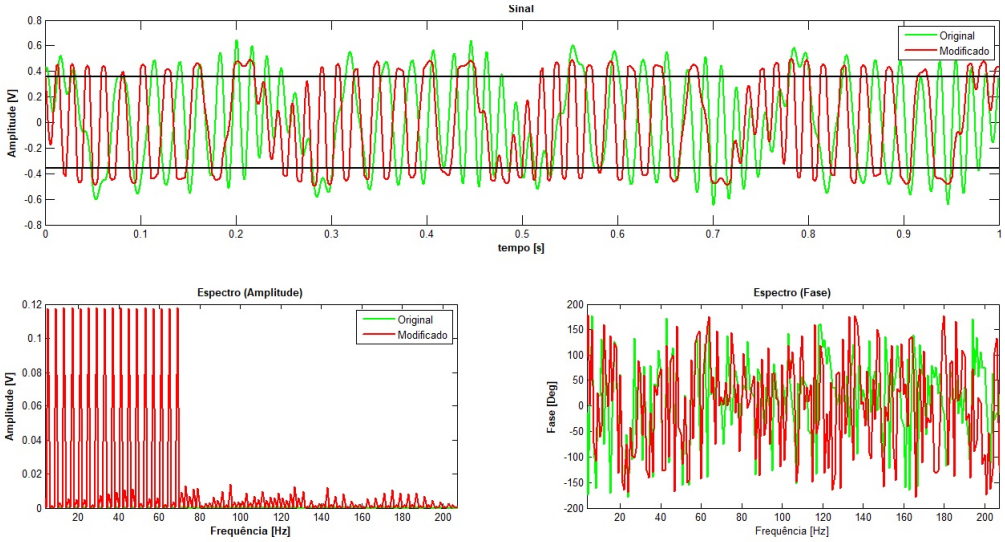

Figure 4: Example of signal modification using the clipping method

4.1 Small scale AMB test rig

The small scale AMB test rig (see Fig. (7)), developed in the Acoustics and Vibrations Laboratory (LAVI) of Federal University of Rio de Janeiro, has an eight pole heteropolar configuration, and supports currents up to 4A, sufficient to levitate a shaft with mass of 1 kg, and is controlled by a decentralized PID algorithm implemented in a FPGA target. Its instrumentation is described in detail in Diaz *et al.* (2017). Some of parameters are presented in Tab. 2.

4.2 Stiffness and Damping estimation results

In order to obtain the equivalent stiffness and damping coefficients of the AMB system, the shaft was shaked first in the horizontal direction and then in the vertical. For each excitation signal, a number of 10 blocks were measured. An example for one experiment is presented in Fig. (8), where the excitation signal, which is a modified multisine using the clipping method with modified spectrum, is applied in the horizontal axis.

The stiffness obtained coefficients, derived from the CDS matrix, are presented in Fig (9). The direct components (i.e. K_{xx} and K_{yy}) are significantly higher than the cross-coupled terms.

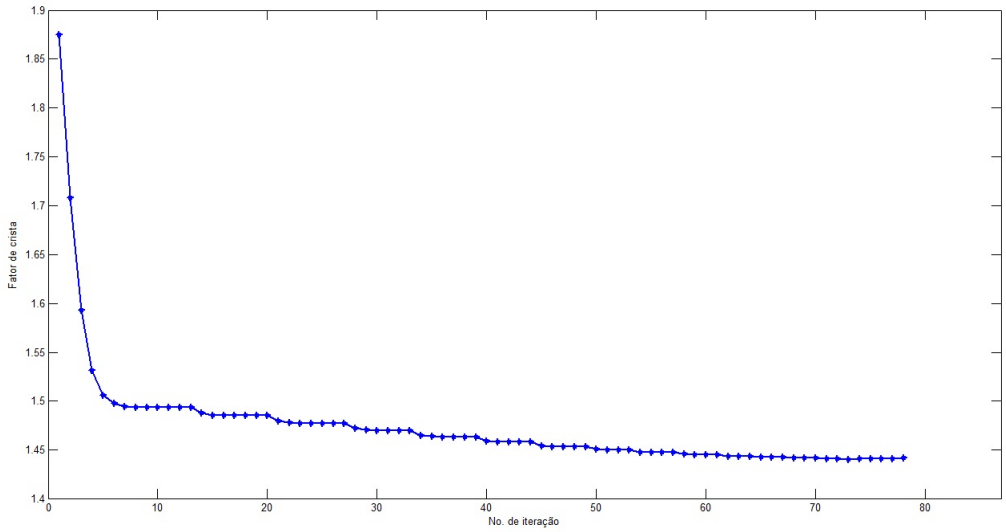

Figure 5: Crest factor evolution for clipping method

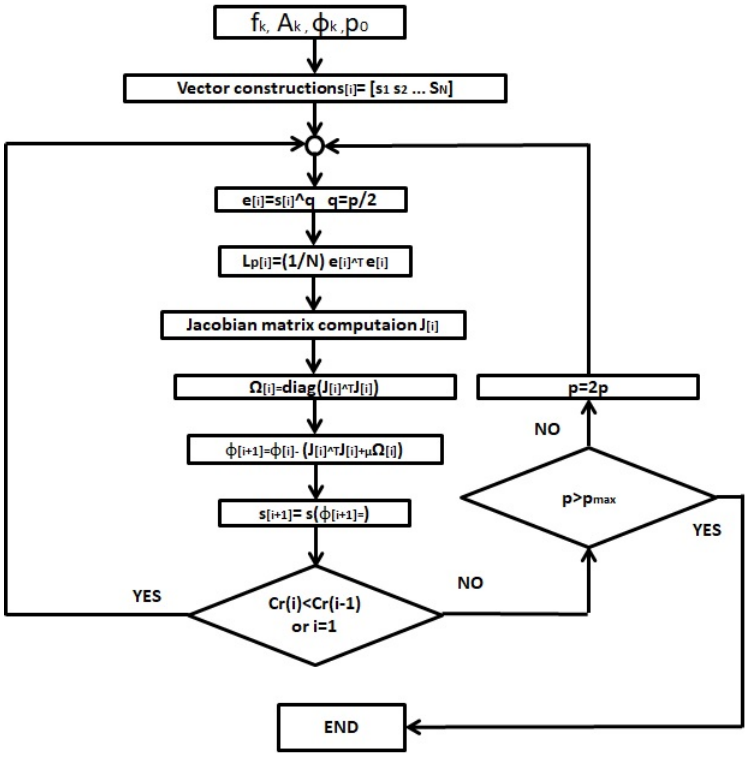

Figure 6: Chebyshev method flow chart (Guillaume *et al.*, 1991)

In the same way, the damping coefficients are estimated, as can be observed in Fig. (10) with relatively low values, indicating the small influence of such parameters.

In order to visualize the uncertainties in the measurements, the standard deviation was computed for the stiffness and damping coefficients, as presented in Fig. (11) and Fig. (12), respectively.

One can observe the low standard deviation values of the stepped sine, and the high uncertainties for the noise and sweep signal. The modified multisine with flat spectrum amplitude performs good only in the low frequencies, since the excitation of the higher frequencies is not as well the modified spectrum signal.

An average of the uncertainties in the excited band frequency is made, and presented in Tab. (3). It can be observed the good performing of the modified multisine signals if compared with the traditional sweep and white noise. The random phase multisine had lower uncertainty values than the modified signal with flat spectrum.

Considering the results obtained by the stepped sine as the *true* coefficients, an error average was computed for each excitation signal, and summarized in Tab. (4). Again, the modified multisine signals with modified spectrum showed the best performance. The modified multisine with flat spectrum presented a higher error

Table 1: Excitation signals assessed in the AMB test rig

	Signal	Spectrum amplitude
1	Stepped sine	
2	Sweep	Flat
3	White noise	
4	Multisine modified by l_p algorithm	Flat
5	Multisine with random phases	Modified
6	Multisine modified by l_p algorithm	Modified
7	Multisine modified by clipping method	Modified

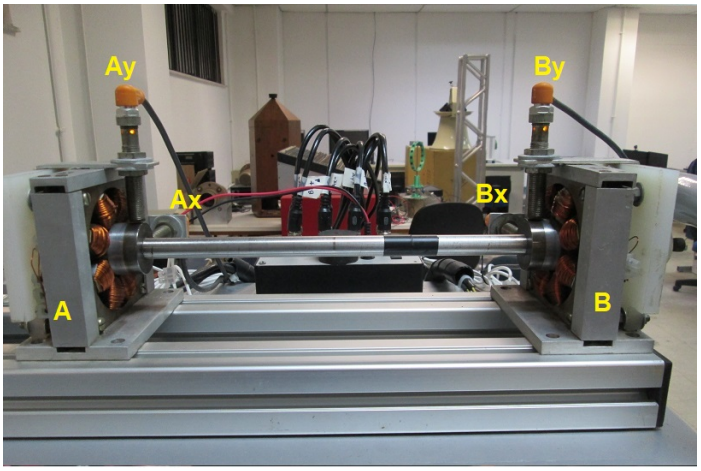

Figure 7: Small scale AMB test rig

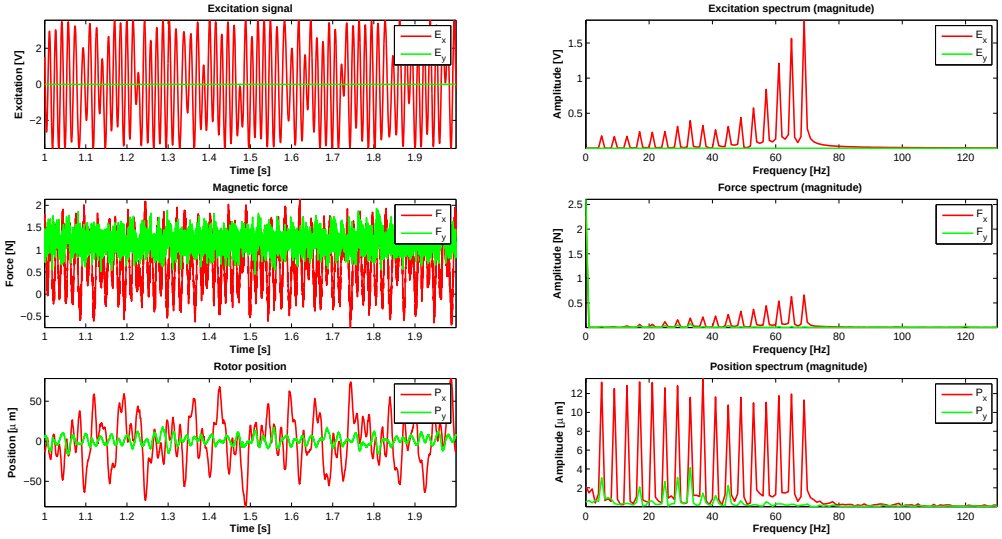

Figure 8: Signal, Magnetic force and Rotor position using Van der Ouderaa *et al.* (1988). Excitation in the horizontal direction

value and the worst scenario were observed for sweep and white noise signal.

5. CONCLUSIONS

The different excitation signals showed that white noise, and sweep performed worse than multisine signals in a previously defined band of frequency, obtained the worst performance, since such signal splits its energy in all frequencies, even out of the established band.

As expected, the stepped sine had the lowest uncertainty, since each frequency was excited at a time. This leads to a total experiment time of approximately 40 minutes, compared to the 40 seconds lasted with each of the other excitation signals assessed.

Table 2: Small Scale T

Parameter		Value	Un.
Shaft mass	m	1	kg
Shaft length	L_s	400	mm
Shaft diameter	d_s	14.28	mm
Journal diameter	d_j	36.4	mm
Distance between actuators	$2a$	315	mm
Distance between sensors	$2c$	36.4	mm
Number of turns	N_v	130	
Bias current	i_b	1	A
Flux Saturation	B_{sat}	1.7	T
Nominal airgap	g_0	1	mm
ÃĄrea seccional do polo	A_g	235	mm^2
Open-loop gain	$K_{mag,x}$	-2.11e4	Nm^{-1}
Actuator gain	$K_{mag,i}$	21.14	NA^{-1}

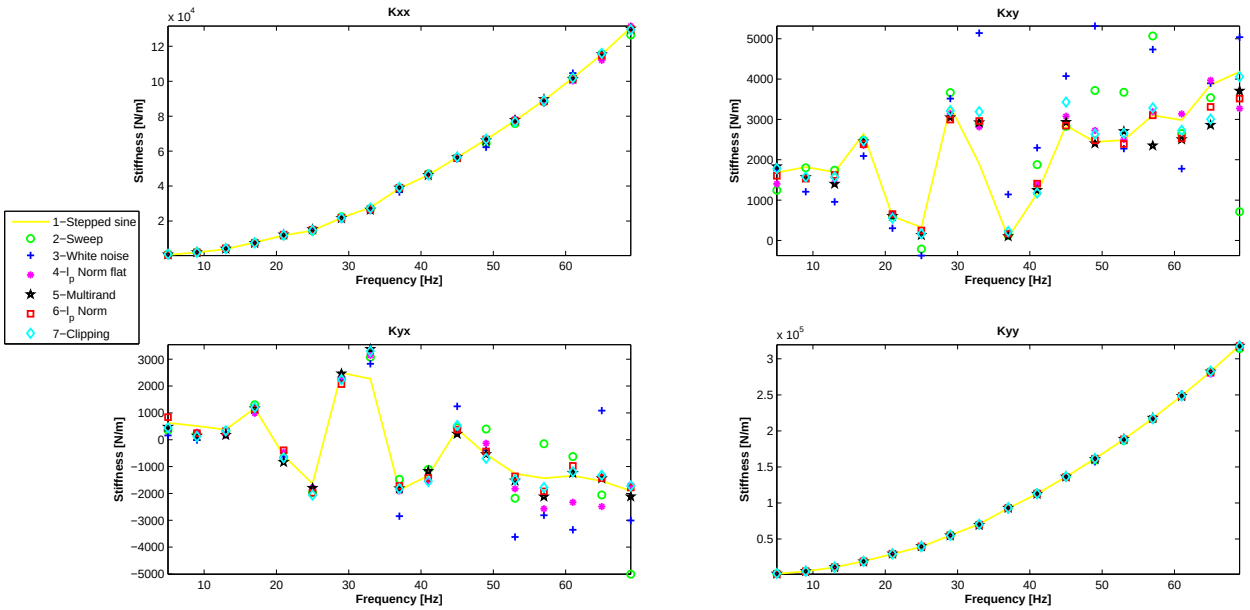

Figure 9: Stiffness estimated coefficients

Not only the crest factor reduction, but also the spectrum distribution is important to obtain adequate results, in order to reduce the uncertainties in the parameters estimation.

As suggestion, the excitation signal design can begin with mapping the spectrum system magnitude (which could be estimate or measured with general purpose excitation signals), and then modified with algorithms as used in this work.

6. ACKNOWLEDGEMENTS

The authors would like to thank CAPES, CNPq and PETROBRAS for the financial support during the research stage.

7. REFERENCES

Diaz, D., Pinto, F., Ritto, T. and Maldonado, D., 2017. "Stepped sine and multisine signal excitation for identification in a small amb test rig". In *Proceedings of the 24th International Congress of Mechanical Engineering*. Curitiba, Brasil, p. 9.

Diaz, D., Pinto, F., Ritto, T., Maldonado, D. and CÃŕrtes, V., 2018. "Nonparametric identification of a small amb test rig at several rotating speeds". In *Proceedings of the 16th International Symposium on Magnetic Bearings (ISMB 16)*. Pequim, China, p. 7.

Guillaume, P., 1992. *Identification of Multi-Input Multi-Output Systems Using Frequency-Domain Models*. Ph.D. thesis, Vrije Universiteit Brussel, Buxelas, BÃĺlgium.

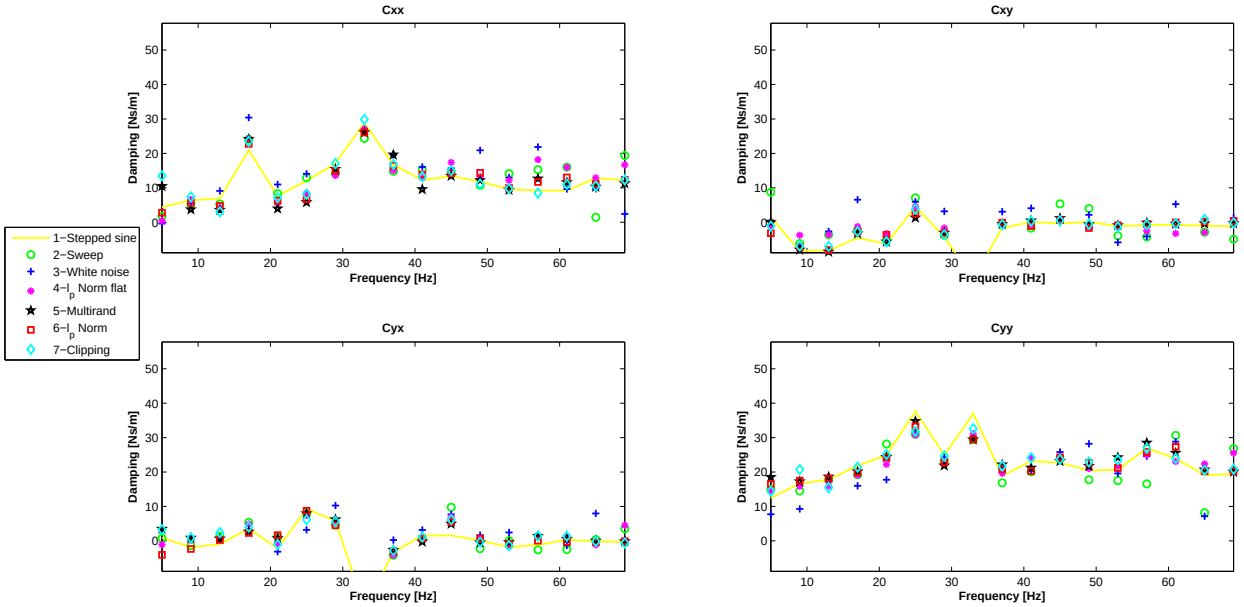

Figure 10: Damping estimated coefficients

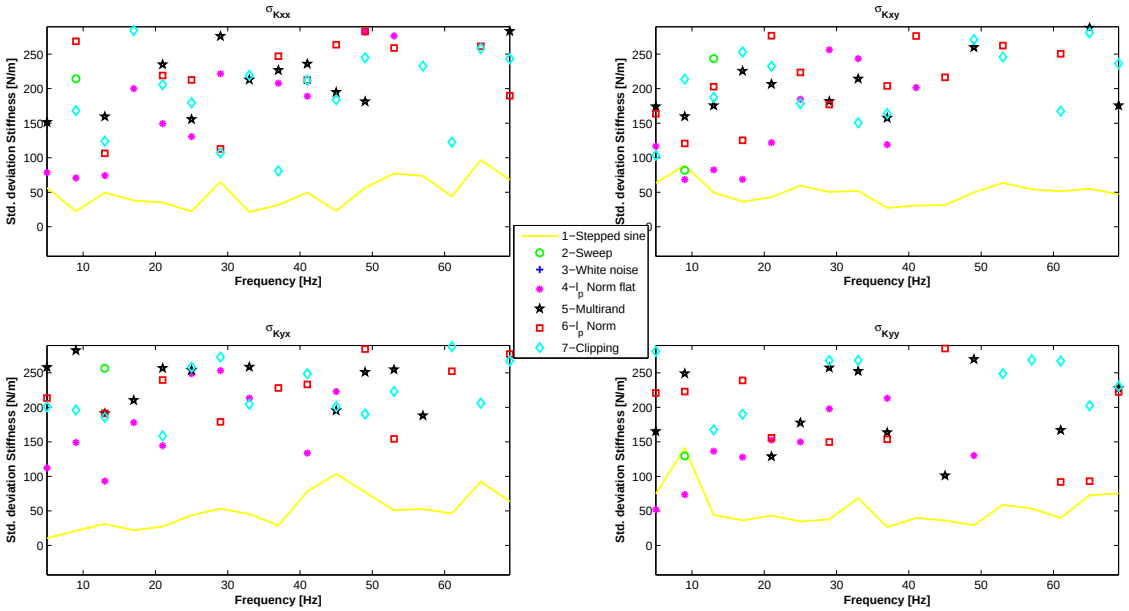

Figure 11: std stiffness

Guillaume, P., 1998. "Frequency response measurements of multivariable systems using nonlinear averaging techniques". *IEEE Transactions on Instrumentation and Measurement*, Vol. 47, pp. 796–800.

Guillaume, P., Schoukens, J., Pintelon, R. and Kollar, I., 1991. "Crest-factor minimization using nonlinear Chebyshev approximation methods". *IEEE Transactions on Instrumentation and Measurement*, Vol. 40, No. 6, pp. 982–989.

Hynynen, K., 2011. *Broadband Excitation in the System Identification of Active Magnetic Bearing Rotor Systems*. Ph.D. thesis, Lappeenranta University of Technology, Lappeenranta, Finlandia.

ISO, 2006. "Mechanical vibration – vibration of rotating machinery equipped with active magnetic bearings – part 3: Evaluation of stability margin". Technical Report ISO 14839-3:2006, International Organization for Standardization.

Khader, S., Liu, B. and SjÃűberg, J., 2014. "System identification of active magnetic bearing for commissioning".

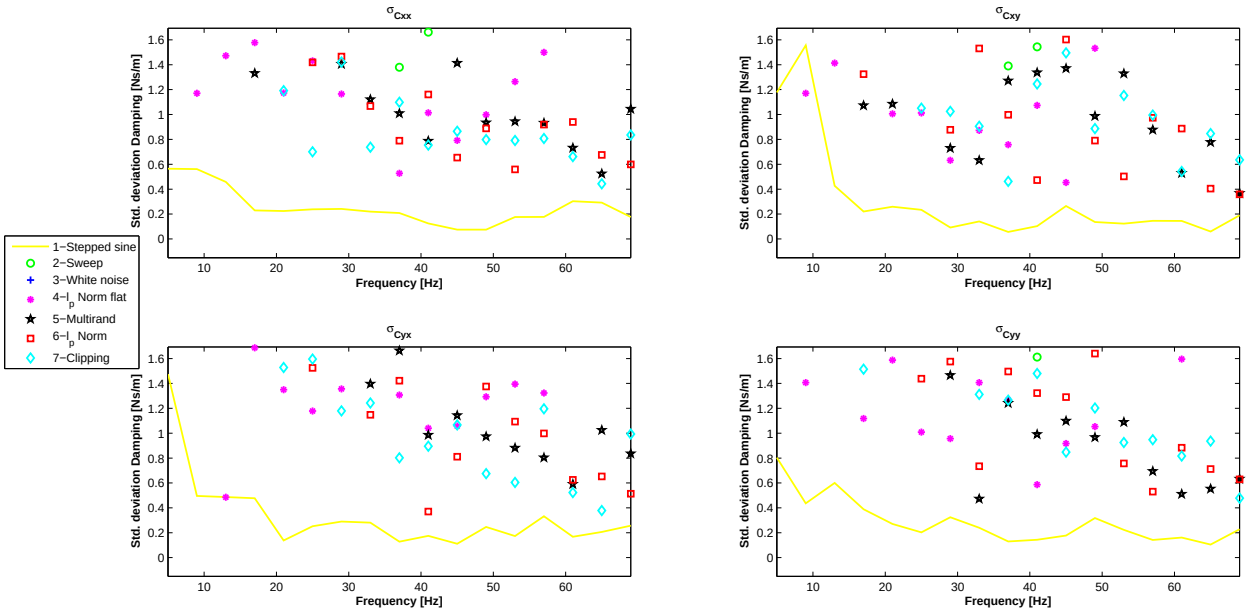

Figure 12: std damping

Table 3: Standard deviation average for stiffness and damping coefficients

Excitation signal	σ_{Kxx}	σ_{Kxy}	σ_{Kyx}	σ_{Kyy}	σ_{Cxx}	σ_{Cxy}	σ_{Cyx}	σ_{Cyy}
	N/m	N/m	N/m	N/m	Ns/m	Ns/m	Ns/m	Ns/m
1- Stepped sine	48.81	50.20	49.8	53.6	0.256	0.313	0.33	0.28
2- Sweep	1.01e3	1.48e4	1.03e3	1.48e4	4.31	5.56	4.331	5.65
3- White noise	5.20e3	4.0611e3	4.05e3	6.32e3	22.6	16.65	19.47	22.39
4- Modified multisine flat spectrum	386.32	422.69	540.84	471.79	1.78	1.81	1.95	1.69
5- Multisine random phase	261.02	265.53	273.87	241.97	2.07	1.54	2.06	1.75
6- Modified with Chev. norm	255.15	252.81	268.74	270.53	2.23	1.41	1.91	1.95
7- Modified by clipping	210.5013	239.73	243.56	299.0376	1.64	1.44	1.74	1.61

In *Proceedings of International Conference on Modelling, Identification and Control*. Melbourne, AustrÃąlia, pp. 289–294.

Muszynska, A., 2005. *Rotordynamics*. Mechanical Engineering. CRC Press.

Nordmann, R., 1984. *Identification of Modal Parameters on Rotors*, CISM Courses and Lectures No. 273, Harburgo, Alemanha, chapter 4.3.

Pintelon, R. and Schoukens, J., 2001. "Measurement of frequency response functions using periodic excitations, corrupted by correlated input/output errors". *IEEE Transactions on Instrumentation and Measurement*, Vol. 50, pp. 1753–1760.

San Andres, L., 2006. "Annular pressure seals and hydrostatic bearings". Technical report, Turbomachinery Laboratory Texas A&M University College Station.

Schoukens, J., Pintelon, R. and Rolain, Y., 2000. "Broadband versus stepped sine frf measurements". *IEEE Transactions on Instrumentation and Measurement*, Vol. 49, pp. 275–278.

Schoukens, J., Pintelon, R., van der Ouderaa, E. and Renneboog, J., 1988. "Survey of excitation signals for fft based signal analyzers". *IEEE Transactions on Instrumentation and Measurement*, Vol. 37, pp. 342–352.

Schweitzer, G. and Maslen, E., 2009. *Magnetic Bearings. Theory, Design and Application to Rotating Machinery*. Springer.

Van der Ouderaa, E., Schoukens, J. and Renneboog, J., 1988. "Peak factor minimization of input and output signals of linear systems". *IEEE Transactions on Instrumentation and Measurement*, Vol. 37, pp. 207–211.

Verboben, P., 2002. *Frequency-Domain System Identification for Modal Analysis*. Ph.D. thesis, Vrije Universiteit Brussel, Buxelas, BÃlgium.

Vuojolainen, J., Nevaranta, N., Jastrzebski, R. and PyrhÃűnen, O., 2017. "Comparison of excitation signals in active magnetic bearing system identification". *Modeling, Identification and Control (MIC)*, Vol. 38, p. 11.

Wernholt, E. and Moberg, S., 2008. "Experimental comparison of methods for multivariable frequency response function estimation". In *Proceedings of the 17th World Congress The International Federation of Automatic*

Table 4: Error average coefficients taking as reference the stepped sine signal

Excitation signal	K_{xx}	K_{xy}	K_{yx}	K_{yy}	C_{xx}	C_{xy}	C_{yx}	C_{yy}
	N/m	N/m	N/m	N/m	Ns/m	Ns/m	Ns/m	Ns/m
2- Sweep	791.09	699.47	609.53	791.09	3.57	3.53	2.37	4.35
3- White noise	1.08e3	981.03	819.89	1.08e3	4.41	4.42	5.11	4.53
4- Modified multisine flat spectrum	713.52	262.16	399.83	713.51	3.05	2.13	2.11	2.51
5- Multisine random phase	404.33	325.33	237.90	404.33	2.66	1.05	1.78	2.31
6- Modified with Chev. norm	405.02	255.82	258.13	405.03	1.88	1.41	1.68	2.19
7- Modified by clipping	299.17	279.63	241.91	299.17	1.79	0.91	1.77	1.91

Control. Seoul, Korea, pp. 15359–15366.

8. RESPONSIBILITY NOTICE

The authors are the only responsible for the printed material included in this paper.